

# Hybrid Spoof Surface Plasmon Polariton and Substrate Integrated Waveguide Broadband Bandpass Filter With Wide Out-of-Band Rejection

Peng Chen , Member, IEEE, Luping Li, Kai Yang, and Qiang Chen, Senior Member, IEEE

**Abstract**—This letter presents a novel hybrid spoof surface plasmon polariton (SSPP) and substrate integrated waveguide (SIW) filter, which has the broadband bandpass and wide out-of-band rejection features. The lower and upper cutoff frequencies of the passband can be independently adjusted by changing the structural parameters of the SSPP and SIW units, respectively. The dispersion curves of the SSPP and SIW units are analyzed and the influences of some structural parameters are investigated. A hybrid SSPP-SIW filter is fabricated based on the proposed method, and the measured passband is at 7.3–11.2 GHz with a relative bandwidth of 44%. The upper stopband rejection level is lower than  $-40$  dB from 11.8 to 19.8 GHz.

**Index Terms**—Broadband bandpass filter, spoof surface plasmon polariton (SSPP), substrate integrated waveguide (SIW).

## I. INTRODUCTION

SUBSTRATE integrated waveguide (SIW) filters are considered as promising candidates for next-generation communication systems as their low-insertion loss, easy manufacture, and flexible integration with other circuits merits [1]. Traditional SIW filters often suffer narrow passband and poor out-of-band rejection limitations. Some efforts have been made to broaden the passband bandwidth [2]–[5]. Considering the broadband ability of the spoof surface plasmon polariton (SSPP) structure [6], researchers have merged the SSPP structure into the SIW filter and termed it as the hybrid SSPP-SIW filter.

The SSPP is a kind of artificial periodic structure to imitate the capability of the natural SPP, which can confine the electromagnetic wave with miniaturized circuit size [6]. The SSPP along with the conversion structure, which converts the electromagnetic mode from the SSPP to spatial mode, can perform a broad passband feature [7], [8]. However, the hybrid SSPP-SIW filter has a better rolloff factor and in-band rejection [9]–[12].

Manuscript received July 29, 2018; accepted August 28, 2018. Date of publication September 24, 2018; date of current version November 6, 2018. This work was supported in part by the National Natural Science Foundation of China under Grant 61601088 and Grant 61571093 and in part by the Fund of Department of Education of Sichuan Province under Grant 18ZB0230. The work of P. Chen was supported by China Scholarship Council through Visiting Scholar Scholarship. (Corresponding author: Peng Chen.)

P. Chen, L. Li, and K. Yang are with the School of Aeronautics and Astronautics, University of Electronic Science and Technology of China, Chengdu 611731, China (e-mail: chenp@uestc.edu.cn; lplees@outlook.com; kyang@uestc.edu.cn).

Q. Chen is with the Graduate School of Engineering, Tohoku University, Sendai 980-8579, Japan (e-mail: chenq@ecei.tohoku.ac.jp).

Color versions of one or more of the figures in this paper are available online at <http://ieeexplore.ieee.org>.

Digital Object Identifier 10.1109/LMWC.2018.2869290

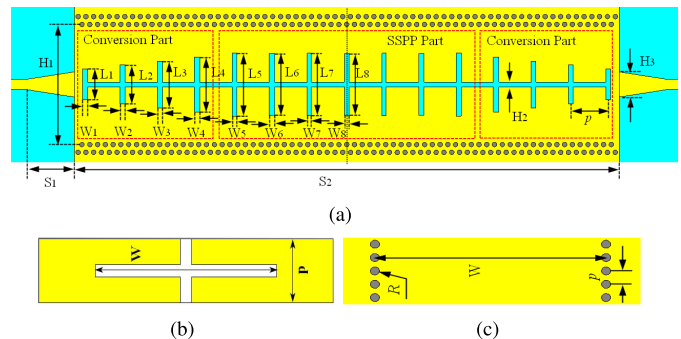


Fig. 1. Top view of the proposed hybrid SSPP-SIW filter. (a) Whole structure. (b) SPP unit (anticlockwise  $90^\circ$  rotation). (c) SIW unit (anticlockwise  $90^\circ$  rotation).

The first hybrid SSPP-SIW filter is bulky as the direct connection of the SSPP and SIW by a pair of tapered microstrip lines [9]. Another one etches different height array transverse metallic blind holes between the two rows metallic via holes [10]. A planar hybrid SSPP-SIW filter is demonstrated but no experimental verification is given [11]. Guan *et al.* [12] introduces a hybrid SSPP half-mode SIW filter. However, none of these hybrid SSPP-SIW filters consider the out-of-band rejection.

A novel hybrid SSPP-SIW filter is proposed in this letter. It simultaneously has broadband bandpass and wide out-of-band rejection. The dispersions of the SSPP and SIW units are discussed, and the structural parameters are studied to balance the passband and the out-of-band rejection performance.

## II. DISPERSION OF SSPP AND SIW UNIT

The proposed hybrid SSPP-SIW filter is illustrated in Fig. 1(a). It can be considered as a combination of the SSPP and the SIW units, which are shown in Fig. 1(b) and (c), respectively. A frequency domain solver from CST microwave studio is employed to investigate the dispersion and analyze the performance of the proposed filter.

The SSPP unit dispersion curves are displayed in Fig. 2(a). These curves remain in the slow wave region, which are similar to the natural SPP material. The cutoff frequency decreases when the length of the slot increases. The wavenumber of the SSPP unit is greater than that of the microstrip line, which suggests the SSPP unit has better electromagnetic constrain, lower coupling, and lower signal crosstalk than the microstrip line.

The SIW unit dispersion curves are subsequently displayed in Fig. 2(b). The SIW unit is in the fast wave region.

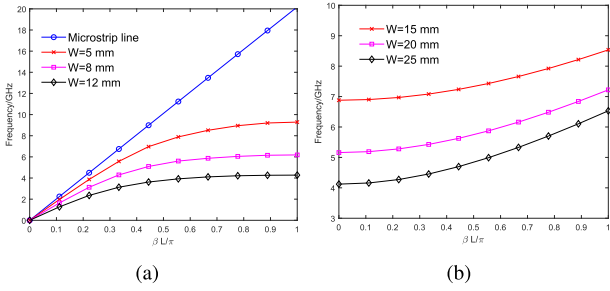


Fig. 2. Dispersion diagrams. (a) SSPP unit. (b) SIW unit.

Besides, the cutoff frequency decreases with the increase of the distance between the two rows metallic via holes, which suggests it has high-pass feature as there exists the lowest cutoff frequency.

According to the two dispersion curves, the combination of the SSPP and SIW unit has the ability to create a bandpass filter if the cutoff frequency of the SIW unit is greater than that of the SSPP unit. It is transparent that the upper sideband of the combination filter is determined by the SSPP unit while the lower sideband is determined by the SIW unit.

III. HYBRID SSPP-SIW FILTER DESIGN

A 7–11 GHz hybrid SSPP-SIW filter will be designed. The distance of the two rows metallic via holes of the SIW unit is set as 15 mm while the length of the vertical slot of the SSPP unit is set as 8 mm based on the dispersion curves in Fig. 2. The traditional trapped microstrip lines are used to connect the input–output 50-Ω microstrip lines as their broadband virtue. The conversion parts with gradually changing heights of the vertical slots are crucial for the final performance. Their values need to be optimized.

Increasing the length of the SSPP vertical slots will make the upper cutoff frequency lower, as shown in Fig. 3(a), while increasing the distance of the two rows metallic via holes will make the lower cutoff frequency shift to the left, as shown in Fig. 3(b). The dispersion curves can precisely predict the upper and lower cutoff frequencies. However, when the lower sideband cutoff frequency of the SIW unit becomes lower, the upper stopband rejection speedily deteriorates. It mainly attributes to the attenuated coupling between the SSPP and SIW units, which makes the whole filter less control of the out-of-band rejection. Therefore, it is quite important to select the proper SSPP unit along with the conversion parts to merge into the SIW unit to extend the out-of-band rejection.

The central horizontal slot could strengthen the upper stopband spurious suppression and broaden the passband about 200 MHz, as shown in Fig. 4(a). Also, it brings an additional transmission zero at the lower stopband to sharp better rolloff factor. Similarly, the widths of the vertical slots will influence the bandwidth and the upper stopband rejection, which is given in Fig. 4(b). Therefore, all of the widths of the vertical slots are treated as design parameters in the final optimization process.

The simulated electric-field distributions of the proposed hybrid SSPP-SIW filter are shown in Fig. 5. It is clear that only the signals in the designed passband can propagate through the hybrid SSPP-SIW filter. According to Fig. 5(d), the energies are highly localized and mainly propagate along the interface

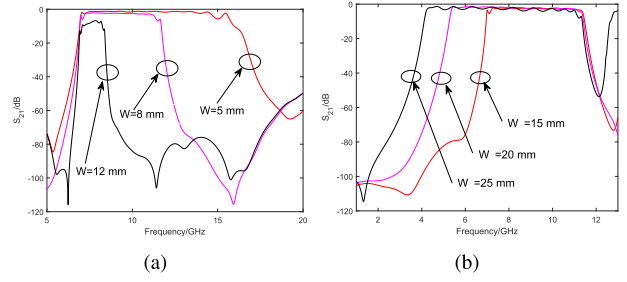


Fig. 3. Simulated transmission coefficients ( $S_{21}$ ) of the filter with (a) different vertical slot lengths and (b) different via heights.

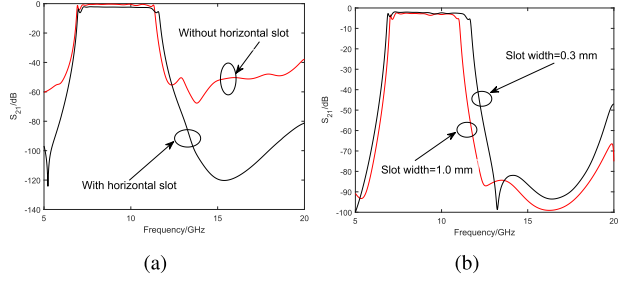


Fig. 4. Simulated transmission coefficients ( $S_{21}$ ) of the filter (a) with/without central horizontal slot and (b) with different vertical slot widths.

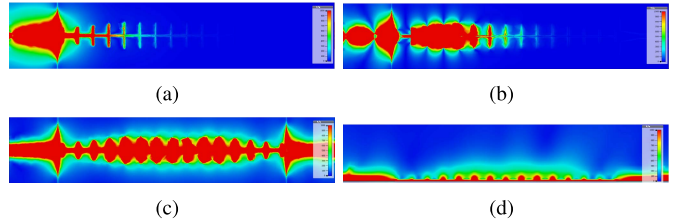


Fig. 5. Simulated electric field distributions of hybrid SSPP-SIW filter. (a) Top view at lower frequency stopband (6 GHz). (b) Top view at upper frequency stopband (13 GHz). (c) Top view at the passband (9 GHz). (d) Side view at the passband (9 GHz).

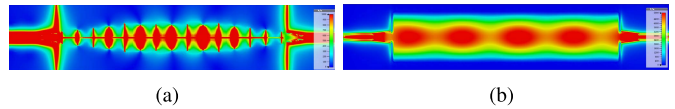


Fig. 6. Simulated electric field distributions at 9 GHz. (a) SSPP unit. (b) SIW unit.

between the air and the metal, which are similar to the natural SPP material. The electric field distributions of the SSPP and SIW units are also displayed in Fig. 6 for comparison. It is remarkable that the mode in the proposed filter is a mixture of the SSPP and SIW modes.

IV. FABRICATION AND MEASUREMENTS

A hybrid SSPP-SIW filter based on the substrate with dielectric coefficient of 2.2 and height of 0.508 is designed, optimized, and fabricated to verify the above-mentioned method. The size is 100 mm × 20 mm. Just as exhibited in Fig. 7, the filter is centrosymmetric and only the left-side parameters are given in Table I, where  $L_i$  and  $W_i$  are the length and width of the vertical slots,  $H_1$  is the height of

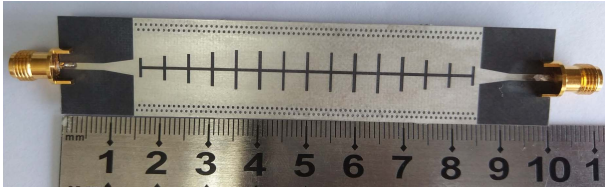


Fig. 7. Fabrication of the proposed SSPP-SIW filter.

TABLE I  
DESIGN PARAMETERS (UNIT: MILLIMETER)

$L_1$	$L_2$	$L_3$	$L_4$	$L_5$	$L_6$	$L_7$	$L_8$
3.96	5.03	6.00	7.04	8.11	7.92	8.00	7.89
$W_1$	$W_2$	$W_3$	$W_4$	$W_5$	$W_6$	$W_7$	$SW_8$
0.62	0.63	0.63	0.70	0.63	0.71	0.52	0.61
$H_1$	$H_2$	$H_3$	$S_1$	$S_2$	$p$		
15.4	0.59	3.23	6.00	70.0	4.80		

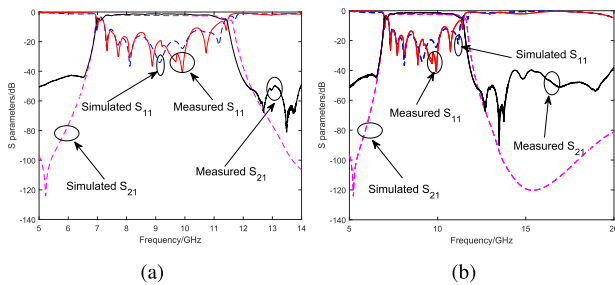


Fig. 8. Measured and simulated reflection coefficients ( $S_{11}$ ) and transmission coefficients ( $S_{21}$ ) of the filter. (a) Passband view. (b) Wideband view.

the two arrays via holes,  $H_2$  is the width of horizontal slot,  $S_2$  is the length of the SSPP part,  $p$  is the period of the slot, and  $H_3$  and  $S_1$  are the width and length of the trapezium matching microstrip line, respectively. Besides, the diameter of the metallic via hole is 0.6 mm and the period of the via holes is 1 mm, which satisfy the requirements to propagate the  $TE_{10}$  mode in the SIW structure.

Fig. 8 compares the simulated and measured results obtained from the Ceyear AV3672C vector network analyzer. According to the passband view, the measured central frequency is 9.25 GHz and the passband is 7.3–11.2 GHz with 44% fractional bandwidth. The insertion loss of the passband varies from  $-2$  to  $-1.2$  dB while the return loss varies from  $-37$  to  $-12.2$  dB. Furthermore, the lower stopband transmission zero is at 6.15 GHz and the upper stopband transmission zero is at 12.85 GHz. According to the wideband view,  $S_{21}$  is lower than  $-40$  dB from 11.8 to 19.8 GHz.

Notably, the simulation results agree with the measurement results in the passband while there is some difference between the upper stopband, owing to several factors. The first reason is the performances of the SubMiniature version A connectors, which are not as good as expectation in high frequency. The second reason is the used fast reduced model broadband sweeping simulation method for time and computer resource consumption reduction. Also, the fabrication accuracy and measurement equipment noise will deteriorate the final performance.

TABLE II  
STATE-OF-THE-ART PLANAR SIW FILTER

Work	BW/GHz	FBW/%	RL/dB	Upper-band Rejection
Ref. [2]	8.8-16	61.5	10	-48 dB@16.8-20 GHz
Ref. [3]	6.8-10.3	42	11	-20 dB@10.4-15 GHz
Ref. [9]	11.9-21.5	57	10	-40 dB@22.5-30 GHz
Ref. [11]	12-18.3	41	10	-40 dB@20.3-22 GHz
Ref. [12]	8-16	50	12	-7 dB@16.2-17 GHz
This work	7.3-11.2	44	12	-40 dB@11.8-19.8 GHz

The state-of-the-art planar SIW filters are listed in Table II, where BW is the bandwidth and RL is the return loss, respectively.

## V. CONCLUSION

A novel broadband bandpass SIW filter based on the SSPP-SIW structure is proposed, in which upper and lower stopband can be independently adjusted. The dispersion characteristics of the SSPP and SIW units are both analyzed, and the influences of some crucial structural parameters are investigated. A 7–11-GHz hybrid SSPP-SIW filter is designed and fabricated to verify the proposed design method. The agreement between the simulated and measured results indicates that the proposed method is a promising candidate for broadband and wide out-of-band rejection SIW filter design.

## REFERENCES

- [1] X.-P. Chen and K. Wu, "Substrate integrated waveguide filter: Basic design rules and fundamental structure features," *IEEE Microw. Mag.*, vol. 15, no. 5, pp. 108–116, Jul. 2014.
- [2] Z.-C. Hao, W. Hong, J.-X. Chen, X.-P. Chen, and K. Wu, "Compact super-wide bandpass substrate integrated waveguide (SIW) filters," *IEEE Trans. Microw. Theory Techn.*, vol. 53, no. 9, pp. 2968–2977, Sep. 2005.
- [3] R. S. Chen, S.-W. Wong, L. Zhu, and Q.-X. Chu, "Wideband bandpass filter using U-slotted substrate integrated waveguide (SIW) cavities," *IEEE Microw. Wireless Compon. Lett.*, vol. 25, no. 1, pp. 1–3, Jan. 2015.
- [4] L. Huang, H. Cha, and Y. Li, "Compact wideband ridge half-mode substrate integrated waveguide filters," *IEEE Trans. Microw. Theory Techn.*, vol. 64, no. 11, pp. 3568–3579, Nov. 2016.
- [5] R. Moro, S. Moscato, M. Bozzi, and L. Perreggini, "Substrate integrated folded waveguide filter with out-of-band rejection controlled by resonant-mode suppression," *IEEE Microw. Wireless Compon. Lett.*, vol. 25, no. 4, pp. 214–216, Apr. 2015.
- [6] X. Shen, T. J. Cui, D. F. Martin-Cano, and J. Garcia-Vidal, "Conformal surface plasmons propagating on ultrathin and flexible films," *Proc. Nat. Acad. Sci. USA*, vol. 110, no. 1, pp. 40–45, Jan. 2013.
- [7] H. F. Ma, X. Shen, Q. Cheng, W. X. Jiang, and T. J. Cui, "Broadband and high-efficiency conversion from guided waves to spoof surface plasmon polaritons," *Laser Photon. Rev.*, vol. 8, no. 1, pp. 146–151, Nov. 2013.
- [8] Z. Liao, J. Zhao, B. C. Pan, X. P. Shen, and T. J. Cui, "Broadband transition between microstrip line and conformal surface plasmon waveguide," *J. Phys. D, Appl. Phys.*, vol. 47, no. 31, p. 315103, Jul. 2014.
- [9] Q. Zhang, H. C. Zhang, H. Wu, and T. J. Cui, "A hybrid circuit for spoof surface plasmons and spatial waveguide modes to reach controllable band-pass filters," *Sci. Rep.*, vol. 5, Nov. 2015, Art. no. 16531.
- [10] D.-F. Guan, P. You, Q. Zhang, K. Xiao, and S. W. Yong, "Hybrid spoof surface plasmon polariton and substrate integrated waveguide transmission line and its application in filter," *IEEE Trans. Microw. Theory Techn.*, vol. 65, no. 12, pp. 4925–4932, Dec. 2017.
- [11] K. Rudramuni, K. Kandasamy, A. Kandwal, and Q. Zhang, "Compact bandpass filter based on hybrid spoof surface plasmon and substrate integrated waveguide transmission line," in *Proc. IEEE Elect. Design Adv. Packag. Syst. Symp.*, Haining, China, Dec. 2017, pp. 1–3.
- [12] D.-F. Guan, P. You, Q. Zhang, Z. B. Yang, H. Liu, and S. W. Yong, "Slow-wave half-mode substrate integrated waveguide using spoof surface plasmon polariton structure," *IEEE Trans. Microw. Theory Techn.*, vol. 66, no. 6, pp. 2946–2952, Jun. 2018.